Research Article Vol. 5, No. 2 / February 2018 / Optica 138

Long-distance telecom-fiber transfer of a radio-frequency reference for radio astronomy

Yabai He,[1,2] Kenneth G. H. Baldwin,[3] Brian J. Orr,[2,*] R. Bruce Warrington,[1] Michael J. Wouters,[1] Andre N. Luiten,[4] Peter Mirtschin,[5] Tasso Tzioumis,[5] Chris Phillips,[5] Jamie Stevens,[5] Brett Lennon,[5] Scott Munting,[5,†] Guido Aben,[6] Thomas Newlands,[6] and Tim Rayner[6]

[1]National Measurement Institute, Sydney, NSW 2070, Australia
[2]MQ Photonics Research Centre, Department of Physics and Astronomy, Macquarie University, Sydney, NSW 2109, Australia
[3]Research School of Physics and Engineering, The Australian National University, Canberra, ACT 2601, Australia
[4]Institute for Photonics and Advanced Sensing, The University of Adelaide, SA 5005, Australia
[5]CSIRO Astronomy and Space Science, PO Box 76, Epping, NSW 1710, Australia
[6]Australia's Academic and Research Network (AARNet), Canberra, ACT 2601, Australia
*Corresponding author: brian.orr@mq.edu.au

Received 1 September 2017; revised 8 November 2017; accepted 8 December 2017 (Doc. ID 306118); published 1 February 2018

Very-long-baseline interferometry (VLBI) for high-resolution astronomical imaging requires phase-stable frequency references at widely separated radio-telescope antennas. For the first time to our knowledge, we have disseminated a suitable radio-frequency (RF) reference for VLBI over a "real-world" telecom optical-fiber link between radio telescopes that are >100 km apart, by means of an innovative phase-conjugation technique. Bidirectional optical amplification is used in parallel with live traffic, and phase perturbations in the effective optical-fiber path length are compensated. This RF-over-fiber approach obviates the need for separate hydrogen masers at each antenna, offering significant advantages for radio-astronomy facilities such as the Square Kilometer Array.

OCIS codes: (060.0060) Fiber optics and optical communications; (060.5625) Radio frequency photonics; (120.3930) Metrological instrumentation; (120.5050) Phase measurement; (350.1270) Astronomy and astrophysics.

https://doi.org/10.1364/OPTICA.5.000138

1. INTRODUCTION

It has long been recognized [1–6] that, in order to transmit stable frequency references over long-distance optical fibers, it is essential to compensate phase perturbations due to various environmental factors. These compensation techniques are often based on returning a light signal along the optical path, then measuring and correcting for the resulting phase shift. Phase-shift compensation has been developed using active variation of the optical path length (e.g., by a fiber stretcher [7,8]), as well as passive compensation techniques. Perturbations on timescales shorter than the round-trip time (RTT) through the optical fiber (RTT ≈ 1 ms/100 km) cannot be directly corrected.

Notable recent fiber-based applications include high-precision phase-coherent optical-frequency transfer for clock networks and high spectral purity [9–17]. Highly stable transfer is also important in the radio-frequency (RF) domain (3 kHz–300 GHz) [7,18,19], where robust RF-over-fiber (RFOF) schemes [20] have been demonstrated by ourselves [21–24] and others [8,19,25–54]. For radio astronomy, long- distance RFOF techniques have been proposed [7,10,17,48,53–55] to send RF references between widely separated antennas in a very-long-baseline interferometry (VLBI) array, as we have now realized.

Recently [17], a remote atomic-clock reference was transferred from Turin over a 550-km optical-fiber link [10] to a single antenna at an Italian radio telescope. More recent work in Poland [55] has connected an atomic clock and a single antenna (15 km apart at Toruń) to more distant Coordinated Universal Time laboratories in Poznań and Warsaw, using a 345-km optical-fiber link. In the context of the Square Kilometer Array (SKA) [56–59], stabilized microwave frequency-reference transfer has recently been realized over optical fiber, via a 52-km link and a 25-km spool, for phase-coherent access to pairs of antennas up to 4.4 km apart at a single radio-telescope site [54]. Various groups (e.g., in Italy, Finland, and Spain, also SKA) are using Precision Time Protocol/White Rabbit (PTP/WR) methods [60–62] to synchronize radio-telescope timescales with nanosecond (ns)-level accuracy.

In contrast, our research is not concerned with absolute timing. It comprises transfer of a phase-stable frequency reference and provides the first-ever practical demonstration of VLBI with a RF reference disseminated over a "real-world" optical-fiber link (>100 km).

2. EXPERIMENTAL METHODS

A. RFOF Transfer System

The relatively simple, passive, phase-conjugate RFOF technique depicted in Fig. 1 was developed as part of our fiber-based frequency-transfer research program [2,11,21,23,24]. Key details of this RFOF-transfer technique were presented in our earlier paper [22] and referenced in the above-mentioned work from other groups [6,11,20,35–40,42–44,49,50,52–54]. A significant rebuild of our system [22] has subsequently been undertaken to improve its reliability when deployed in a real-world remote environment. This enables cost-effective transfer of RF references over long distances in an optical-fiber link where temperature variation, stress induced by bending, distortion of the optical fiber, etc. give rise to phase fluctuations. Potential applications include VLBI radio astronomy, as reported here.

Our algebraic phase-conjugation method [22] passively compensates slow optical-fiber fluctuations, i.e., those longer than the RTT (~1 ms/100 km). RF signals transmitted as amplitude modulation of the local (master) and remote (slave) lasers (operating at telecom wavelengths of ~1.55 μm) are thereby locked such that the phase difference between them is independent of the optical path length. On timescales shorter than the RTT, the high-quality quartz oscillator (slave RF_S) acts as a "flywheel" at the remote location to serve as a highly stable, free-running frequency source. We have verified this approach in tests over a 150-km urban optical-fiber network without optical amplification [22]. For RFOF transfer over longer distances (as required for VLBI), we need to include bidirectional erbium-doped fiber amplifiers (EDFAs) [6,27,30,31,54,55,63,64] to amplify and pass the RF-modulated laser radiation in both directions. Polarization scramblers have also been employed to randomize the output polarization of the local and remote lasers and the polarization-dependent propagation time through the fiber link.

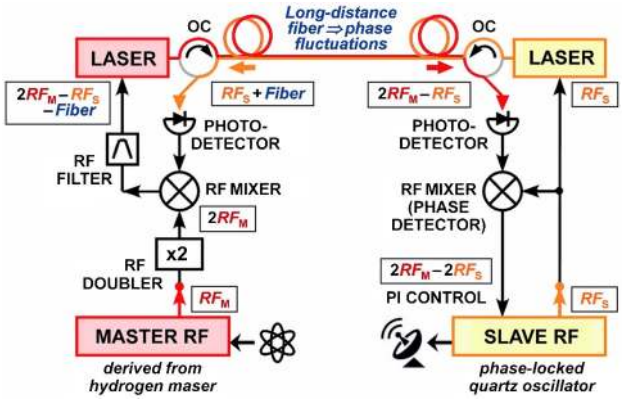

Fig. 1. RFOF transfer schematic. The local (master) and remote (slave) oscillators communicate via a long-distance single-mode optical-fiber link terminated at each end by an optical circulator (OC). The slave laser output is amplitude-modulated at RF_S but experiences phase shifts ("Fiber" in blue) during propagation on the fiber link. The perturbed output (RF_S + Fiber) is difference-frequency-mixed with twice the master frequency ($2RF_M$) to amplitude-modulate the master-laser output. Following retransmission, the fiber phase shift then cancels via algebraic phase conjugation, and the output ($2RF_M - RF_S$) is difference-frequency-mixed with RF_S. The phase difference ($2RF_M - 2RF_S$) is then nulled using a proportional integral (PI) servo to reference the slave to RF_M. Input from the local atomic clock and output to a remote radio-telescope antenna are depicted as icons.

The quartz oscillator is highly stable, with a fractional-frequency Allan deviation $\sigma \approx 2 \times 10^{-13}$ at 1 s—suitable for frequency transfer on continental scales (up to 10,000 km round trip). Our passive RFOF approach thereby maintains long-term phase coherence between two widely separated frequency sources without the additional complexity of actively stabilizing the optical path length, as is necessary in some other RFOF techniques [7,8].

The (local) master and (remote) slave units employ distributed-feedback diode lasers, operating in communications-band channels centered at 1550.92 nm and 1543.73 nm, respectively, and RF-amplitude-modulated to enable frequency transfer. The master signal RF_M at 80 MHz is derived from a 10-MHz reference via a local frequency-synthesizer chain locked to a hydrogen-maser atomic clock. The slave signal RF_S (which provides a reference to a remote antenna) is derived from the stable, low-noise 5-MHz quartz oscillator, then multiplied to 80 MHz and carried over the optical-fiber link. Passive phase conjugation based on frequency mixing is then used to compensate for drifts in the effective length of the optical-fiber link. The high-quality quartz oscillator provides a stable reference signal on timescales less than the RTT, with a servo time constant of ~0.1 s and stability comparable to that of hydrogen masers on ~1-s timescales.

B. Long-Distance Optical-Fiber Link Between Radio Telescopes

For the first time to our knowledge, we have applied our RFOF transfer technique [22] to send a reference frequency between two widely separated radio antennas for VLBI with baseline separations greater than 100 km. In VLBI, two or more antennas separately measure the radio signal from an astronomical source; interferometric combination of the signals then yields enhanced-resolution information about the source's structure and position. VLBI requires a stable RF reference at each location, usually derived from local hydrogen masers that are stable to ~1 part in 10^{15} over several hours [65]. This is costly (typically ~US $200,000/maser), and it constrains reliability when many antennas are used in radio-astronomy facilities such as the SKA [56–59].

To verify that our approach can be used for VLBI without a separate hydrogen maser for each widely separated antenna, we have conducted RFOF transfer experiments under "real-world" conditions between radio-astronomy sites in rural Australia, as depicted geographically in Fig. 2. The two sites—the Australia Telescope Compact Array (ATCA), based ~25 km west of Narrabri (in northwestern New South Wales) and an associated VLBI facility at Mopra (115 km southwest) [65–68]—are connected by 155 km of optical fiber in a buried telecom link (blue in Fig. 2). This link also carries data traffic as part of the Australian Academic Research Network (AARNet), which provides high-speed telecom services for the Australian education and research community. For longer-haul RFOF transfer, the fiber can be looped back at the Mopra telescope site via a second parallel fiber to yield an overall optical-fiber path length of 310 km (red in Fig. 2; see also Fig. 3) between ATCA antennas. These 155-km and 310-km links were used in several radio-astronomy experiments, as described below.

For RFOF transfer over such long distances, optical-fiber losses (approximately 20 dB/100 km) need to be compensated

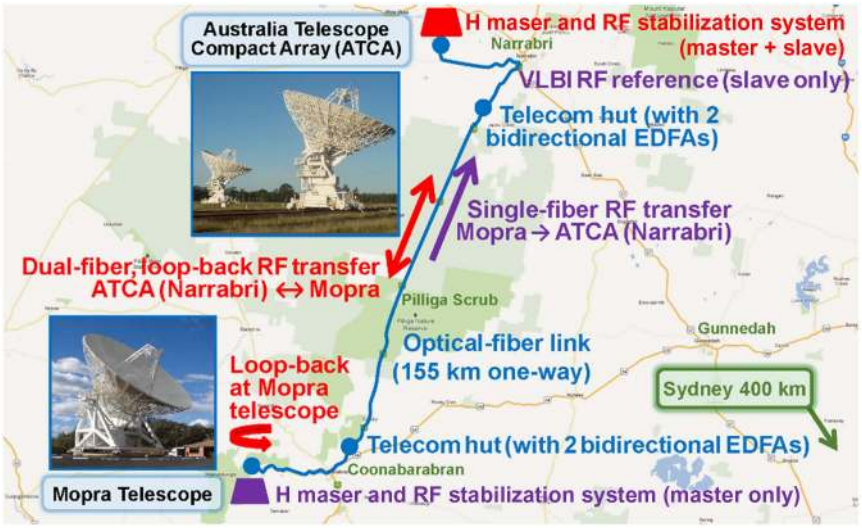

Fig. 2. Layout of VLBI radio-astronomy experiments using RFOF reference transfer. A 155-km AARNET optical-fiber link (blue) connects radio-telescope antennas at ATCA (near Narrabri) and Mopra (near Coonabarabran) via two telecom huts where bidirectional EDFAs are installed. One configuration (purple) transfers the hydrogen-maser reference at Mopra to an ATCA antenna for VLBI demonstrations with a 115-km baseline. Another (red) extends RF transfer over 310 km via a parallel pair of optical fibers looped back at Mopra to test the phase stability of RFOF transfer between a subset of ATCA antennas.

by introducing bidirectional EDFAs [6,27,30,31,54,55,63,64]. Pairs of EDFAs (IDIL Fibres Optiques, each with ∼18-dB gain) were installed by AARNet staff in Controlled Environment Vault telecom huts at Springbrook Creek (south of Narrabri) and at Constellation Avenue (near Coonabarabran). Access to the telecom huts was required to break out one wavelength channel so that the bidirectional EDFAs could be inserted on long-distance dark-fiber segments before combining with other communication signals at other wavelengths.

Reliable operation of the buried optical-fiber link was itself severely challenged by the instability of the black-soil country in the Pilliga Scrub region south of Narrabri. Varying moisture levels sometimes cause the soil to undergo major, rapid expansion and contraction, exerting strong torsional forces that are sufficient to dislodge buried fiber cable. At the time of our RFOF and VLBI experiments, displaced fiber was in some places hung from roadside fences during repair work. Since our earliest experiments, AARNet has improved and rerouted paths of some segments of the fiber link. The unstabilized link was measured to have a relative stability of $\sim 10^{-13}$ on a 1-h timescale, presenting a stringent "real-world" test of the RFOF technique.

C. VLBI Radio Astronomy Experiments

We have used part of the Australian Long Baseline Array facilities [65,67,68], operated by Commonwealth Scientific and Industrial Research Organisation (CSIRO), for VLBI measurements that employ separate simultaneously active radio telescopes for high-resolution astronomical imaging. Specifically, the six radio antennas at ATCA (∼500 km northwest of Sydney) are separated by distances ranging from ∼50 m to 6 km. Each antenna's parabolic surface has a 22-m diameter, as does the single antenna of the Mopra telescope (∼30 km west of Coonabarabran and

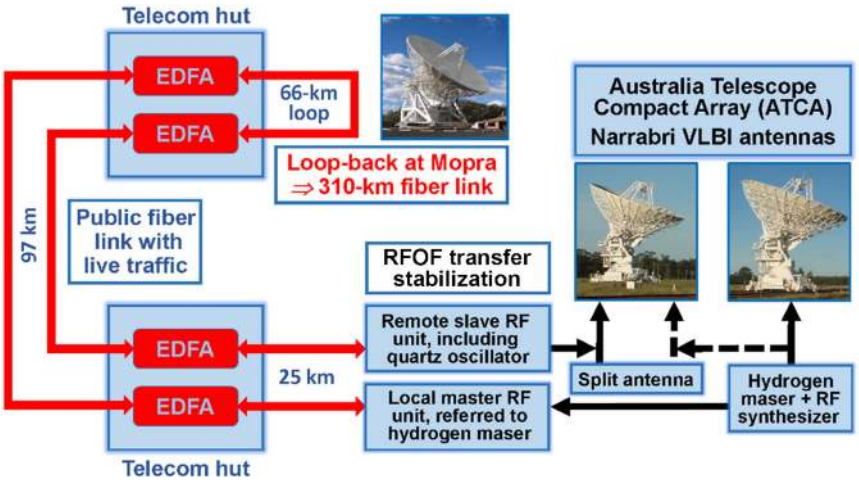

Fig. 3. RFOF loop-back transfer configurations for phase-stability experiments. The RF reference derived from a hydrogen maser at ATCA (Narrabri) is sent to Mopra and looped back to ATCA over a 310-km fiber link (red double-ended arrows). Configurations for the master and slave RF references are shown as black single-headed arrows (dashed for extra connections to the second path of the split antenna).

115 km southwest of the ATCA observatory near Narrabri). Our VLBI studies also included measurements at other more remote radio observatories with their own local hydrogen-maser references (Parkes and Hobart, ~350 km and ~1400 km south of ATCA, respectively), comprising typical configurations for astronomical VLBI observations [65,67,68].

D. RFOF Experiments on Reference Transfer Over the 310-km Link

A key limiting factor in the phase stability of VLBI measurements arises from local atmospheric disturbances at the two antennas. To reduce the influence of atmospheric phase fluctuations and to measure the performance of our frequency-dissemination technique [22,24], we employed the 310-km loop-back link for RFOF transfer via Mopra (Fig. 3; also red in Fig. 2) and performed measurements using only the (closely spaced) ATCA antennas.

In one experiment, atmospheric perturbations were significantly reduced by using two ATCA antennas separated by 77 m (Fig. 3, solid black arrows). The frequency reference for one antenna was provided by a local hydrogen maser at ATCA, while 310-km RFOF transfer via the Mopra loop-back link delivered the transferred reference to the adjacent antenna.

In another key experiment, one of the ATCA radio antennas (Fig. 3, dashed black arrows) was used in a "split-antenna" configuration to virtually eliminate atmospheric perturbations. In this mode of operation (see Ref. [54] for schematic details), the local hydrogen maser provides a reference signal via a frequency-synthesizer chain to one of ATCA's two independent signal-processing paths, while the second path on the same antenna is able use a corresponding reference sent *via* the 310-km RFOF loop-back link.

E. Laboratory Tests of RFOF Performance: Impact of Reference-Frequency Instability

Even if atmospheric fluctuations are removed completely, additional phase perturbations can arise from instabilities in the frequency chain providing the reference frequency RF_M. Laboratory-based experiments therefore explored such effects, using our RFOF transfer system (Fig. 1) operating at 80 MHz with one or two 25-km fiber spools separating the master and slave sections. Use of spooled optical fiber allowed us to avoid complications arising from rapid environmentally induced phase shifts such as those that might occur in the long-distance optical-fiber link.

Triangular, sinusoidal, and square waveforms from a signal generator were employed to simulate phase instability in the master and slave reference frequencies. In regular operation, our RFOF transfer system detects the phase difference between RF_S (slave) and RF_M (master) signals. A proportional-integral (PI) control circuit drives the RF_S slave quartz oscillator and thereby nulls the phase error. In this set of tests, we temporarily replaced the RF_S oscillator signal with the same RF_M and recorded the output of the mixer phase detector for fast and accurate evaluations.

3. RESULTS AND DISCUSSION

A. Measurement of Frequency-Transfer Stability Over the "Real-World" Fiber Link

The performance of our RFOF long-haul transfer technique was assessed in terms of the fractional frequency stability of its RF transfer signal, evaluated by making out-of-loop measurements of signals RF_M and RF_S, using a digital phase meter [21,22]. Figure 4(a) presents Allan deviation plots showing fractional frequency stability $\sigma = (\Delta f/f)$ as a function of averaging time τ. Figures 4(b) and 4(c) show other plots of raw phase and phase-noise spectral density, respectively.

The results in Fig. 4 were measured for RF transfer over the 310-km ATCA–Mopra–ATCA loop-back fiber link (red line, Fig. 2). All of these measurements were undertaken at $f =$ 20 MHz within the frequency-multiplier chains of the RFOF system that ultimately yielded the 80-MHz RFOF transfer signal. Two successive experimental runs (i) and (ii) were made over periods of 29 h (~10^5 s) and 14.5 h (~5×10^4 s), respectively, as indicated in the phase-transfer plots (i) and (ii) in Fig. 4(b). Also, the spectral density plot in Fig. 4(c) corresponds to (i).

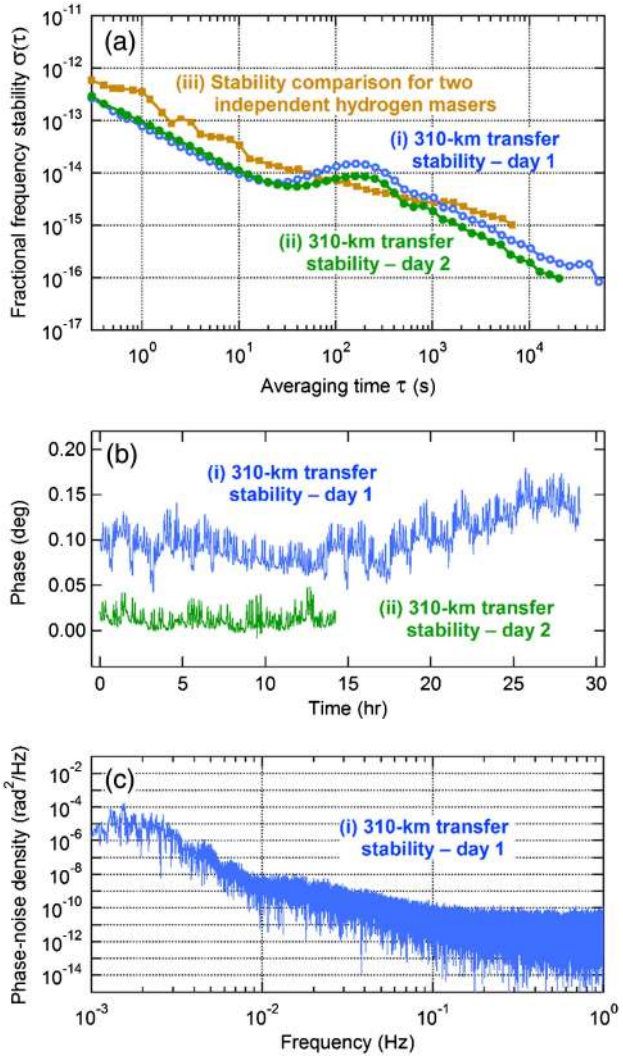

Fig. 4. RFOF transfer performance over the 310-km fiber link. (a) Fractional frequency stability, plotted in the form of Allan deviation σ versus averaging time τ, for two different measurements (i) and (ii) at $f = 20$ MHz over the 310-km ATCA–Mopra–ATCA loop-back fiber link on successive days. Trace (iii) shows the fractional frequency stability at $f = 5$ MHz between two independent hydrogen masers co-located at ATCA. (b) Raw phase-transfer fluctuations versus elapsed time for the same measurements (i) and (ii) on successive days. (c) Phase-noise spectral density versus frequency measured on day 1.

Traces (i) and (ii) of Fig. 4(a) show a fractional frequency stability of $\sigma(\tau) < 10^{-16}$ at the maximum averaging times τ of 5×10^4 s (~14 h) and 2×10^4 s (~5.5 h), respectively. Throughout this study, similar results have been obtained from many other regular measurements not reported here; these verify the day-to-day stability of our RFOF system.

Likewise, trace (iii) of Fig. 4(a) shows the corresponding RF stability between two ATCA-based hydrogen masers, with their 5-MHz output signals measured by means of a digital phase meter [21,22]. Comparison with traces (i) and (ii) of Fig. 4(a) shows RFOF performance that is generally superior to the relative stability of the two hydrogen masers at ATCA. However, a slightly increased instability around $\tau = 200$ s is evident in the Allan deviation plots (i) and (ii).

The phase-transfer plots in Fig. 4(b) show the fluctuations that yield the corresponding Allan deviation plots (i) and (ii) in Fig. 4(a). The peak-to-peak amplitude of short-term phase fluctuations is ~0.05°. A Fourier transform can be used to convert Fig. 4(b) to power spectral density plots such as that shown in Fig. 4(c), which corresponds to the data set (i) for day 1 as in Figs. 4(a) and 4(b). These show persistent fluctuations around a few megahertz (mHz(and are consistent with the excursions at $\tau \approx 200$ s in the Allan deviation plots (i) and (ii) of Fig. 4(a). In Fig. 4(c), the phase noise is as low as ~3.2 μrad/$\sqrt{\text{Hz}}$ (or $\sim 1 \times 10^{-11}$ rad^2/Hz) at frequencies above 0.1 Hz, with greater fluctuations in the region of a few mHz.

As discussed later in this paper, we attribute this to phase fluctuations in the reference RF_M from ATCA's frequency chain, rather than from RFOF transfer over the 310-km optical-fiber link. No such increase in instability was found in our previous laboratory- or field-based tests at other locations [22]. Since our ATCA-based tests shown in Fig. 4(a), similar phase variations have been observed in other tests at ATCA, using different techniques [54].

The Allan deviation plots (i) and (ii) of Fig. 4(a) show that our RFOF transfer method is highly competitive with those for other fiber-based frequency-transfer results [7,19,27,31,38,48], particularly for links longer than 80 km and RF signals of 200 MHz or less. Our fractional stabilities (e.g., $\sigma = 1.0 \times 10^{-16}$ at $\tau \approx 2 \times 10^4$ s over the 310-km link) markedly improve upon the recently reported 8-GHz microwave-frequency transfer performance (5.0×10^{-16} at 1.6×10^4 s over a 166-km metropolitan network) [53] using one technique that is being evaluated for SKA applications. Likewise, other recent ATCA-based frequency-stability measurements [54] over a 77-km fiber link (which included 25 km of spooled fiber) with a maximum antenna separation of 4.4 km yield phase-difference fractional stabilities at $\tau \approx 1 \times 10^4$ s of 9×10^{-16} (for $f \approx 5$ GHz) and 1.1×10^{-16} (for $f \approx 25$ GHz).

B. RFOF-Referenced VLBI Measurements with a 115-km Baseline Separation

Our principal radio-astronomy results demonstrate direct application of our RFOF method to VLBI over a long-haul optical-fiber link, employing just a single hydrogen-maser frequency reference. These RFOF-referenced VLBI measurements were undertaken between the Mopra antenna and one of two antennas (60 m apart, here arbitrarily numbered 1 and 2) 115 km away at the ATCA Narrabri radio telescope (which itself comprises an array of six antennas with a maximum baseline separation of ~6 km). The hydrogen-maser frequency reference was located at Mopra, remote from the ATCA end of the 155-km optical-fiber link (blue line in Fig. 2).

Figure 5 portrays the representative outcome of one such VLBI experiment, performed over a 36-min period. Such VLBI measurements were made simultaneously with each antenna pointing at a strong astronomical source (PKS 0537-441) centered at 8.4 GHz. In Fig. 5, the red trace (i) shows conventional VLBI results between Mopra and Antenna-1 at ATCA, with the frequency reference sourced from the respective local hydrogen masers at both Mopra and ATCA. The corresponding purple trace (ii) was simultaneously recorded using the frequency reference generated at Mopra and transferred by RFOF via the 155-km optical-fiber link to Antenna-2 at ATCA (i.e., with no need for a local reference at ATCA). The origins of the simultaneously recorded phase-transfer plots (i) and (ii) are set arbitrarily to coincide. Their offset depends insignificantly on instrumental factors such as different cable lengths in each channel.

Figure 5 also displays the phase difference (iii) between plots (i) and (ii); this black trace (iii) is arbitrarily displaced downwards by 150°; it has a slowly varying peak-to-peak amplitude of ~40° and a short-term noise level of ±2°. Such variations are typical of regular VLBI observations at ATCA and Mopra. The observed phase difference (iii) here comprises three inseparable components: the relative phase stability of maser-based RF reference frequency chains at both Narrabri and Mopra; the stability of RFOF transfer on the 155-km Mopra-to-Narrabri link; and differential fluctuations in atmospheric conditions viewed by the two Narrabri antennas over the 60-m distance between them. Further experiments (for which results are described below in Sections 3.C and 3.D) indicate that the first and third of these effects are most likely to be dominant here.

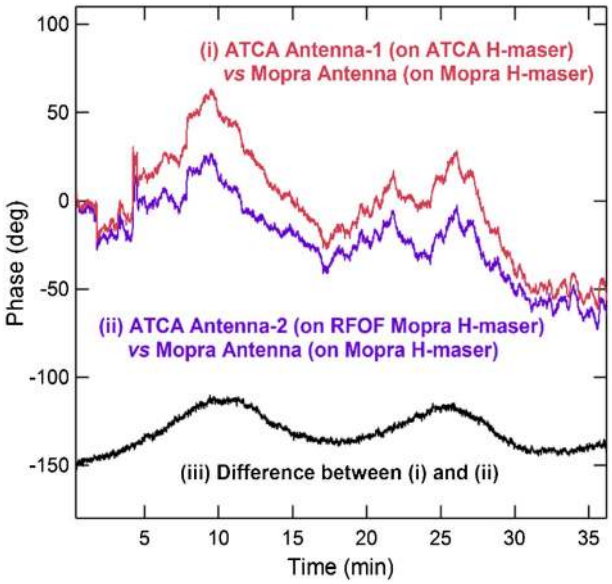

Fig. 5. VLBI measurements demonstrating reference-frequency transfer between pairs of antennas that are 115 km apart. These VLBI measurements at $f \approx 8.4$ GHz involved three radio-astronomy antennas, one at Mopra (with its own local frequency reference) and two at ATCA, with their respective frequency references provided (i) locally at ATCA and (ii) by RFOF transfer from Mopra, via the 155-km fiber link. The phase difference between traces (i) and (ii) is also displayed in trace (iii), arbitrarily displaced downwards by 150°.

C. RFOF Experiments on Reference Transfer Over the 310-km Link

As explained above, to minimize atmospheric phase-fluctuation effects, the 310-km loop-back link via Mopra (Fig. 3; red in Fig. 2) was used for several RFOF-referenced radio-astronomy tests. One such experiment used two adjacent ATCA antennas (77 m apart—solid black arrows in Fig. 3). The phase stability provided by the 310-km link was then found to be indistinguishable from that when both antennas were referenced directly to a single local hydrogen maser.

Another key experiment, with results as in Fig. 6, used one of the ATCA radio antennas (dashed black arrows in Fig. 3) in a "split-antenna" configuration intended to eliminate the effect of atmospheric perturbations. In these experiments, the local hydrogen maser and its frequency chain provided a reference to one of ATCA's two independent signal-processing paths, while the second path on the same antenna used a corresponding reference —*either* local *or* remote (via the 310-km fiber link).

Figure 6 shows the split-antenna results, with only period (b) using 310-km RFOF. For each path in panels (b) and (c) (red and black curves), varying atmospheric conditions yield RF-phase fluctuations that exceed those in panel (a). Nevertheless, the differential signal (black line, middle panel) has no discernible difference between direct and loop-back hydrogen-maser reference signals (apart from constant arbitrary phase offsets which depend on instrumental factors, as explained in the context of Fig. 5). These minor residual differential phase variations cannot be due to atmospheric perturbations as both channels share the same radio antenna and hence the same viewing conditions. However, the phase variations do appear to be correlated with temperature variations (magenta, bottom panel) of inlet cooling air at floor level in the ATCA instrument room where the hydrogen maser and its associated frequency-synthesizer chain are housed.

The maximum magnitude of noise fluctuations in the phase differences (middle panels of Fig. 6) is ~20° peak-to-peak. This is consistent with corresponding peak-to-peak noise levels of ~0.05° observed at $f = 20$ MHz in Fig. 4(b), allowing for the 420× frequency increase (to $f = 8.4$ GHz) in the case of Fig. 6.

The differential phase variations observed in Fig. 6 are evident in all three periods, including periods (a) and (c), where any putative phase contributions from the 310-km RFOF transfer are absent. In all cases (a)–(c), therefore, their most likely cause is attributed to residual phase fluctuations in the RF_M reference supplied by ATCA's frequency chain. These differential phase variations (<10° peak-to-peak, with a dominant period of ~15 min) observed in the split-antenna experiments are consistent with the increased instability seen at $\tau \approx 200$ s in the Allan deviation plots (i) and (ii) of Fig. 4(a). Observed differential phase variations are much smaller than typical atmospheric impacts on VLBI astronomical observations.

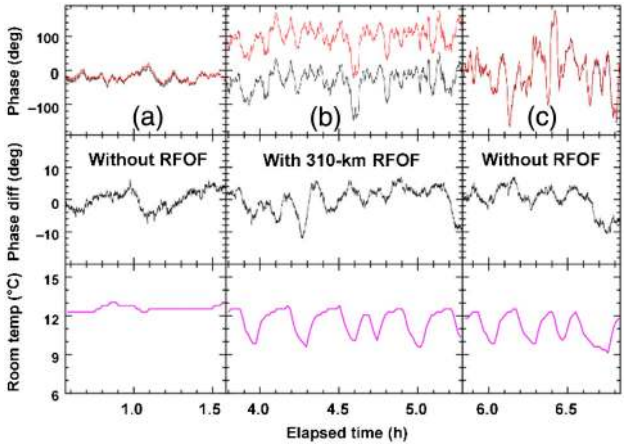

Fig. 6. Phase stability for the split-antenna RFOF experiment. The top panel shows the RF phase variation at $f \approx 8.4$ GHz for the two split-antenna signal-processing paths (red and black) for three successive time periods. Periods (a) and (c): both paths have a local hydrogen-maser reference. Period (b): the red channel uses the reference sent via the 310-km optical-fiber link. The middle panels show the phase difference (on a ~10 × finer scale relative to the top panels) between the two split-antenna paths—with the fixed phase offset between the two period (b) signals removed. The bottom panels show floor-level temperature variations in the ATCA instrument room where the hydrogen maser and associated electronics are housed.

D. Source of Residual Phase Fluctuations

The small persistent residual phase variations noted above had not occurred in previous laboratory- and field-based experiments; they are consistent with the observed increase in the Allan deviation plots (i) and (ii) at $\tau \approx 200$ s in Fig. 4(a). Various measures to isolate the RFOF transfer instrument, undertaken both at ATCA and in our Sydney laboratory, indicated that it was highly stable mechanically, thermally, and electronically. A series of laboratory-based tests were conducted with results as illustrated in Fig. 7. These tests explored whether the observed residual phase fluctuations in the VLBI signals (Fig. 5) and in the RFOF experiments (Figs. 4 and 6) were caused by instability in the reference RF_M itself as generated by ATCA's hydrogen-maser frequency chain. To record Fig. 7, a signal generator was used to simulate phase variations in the (identical) RF_M and RF_S reference signals, with a phase-modulation amplitude of ~400° applied with a half-period of 50 ms (i.e., at a triangle-wave rate of ±8°/ms).

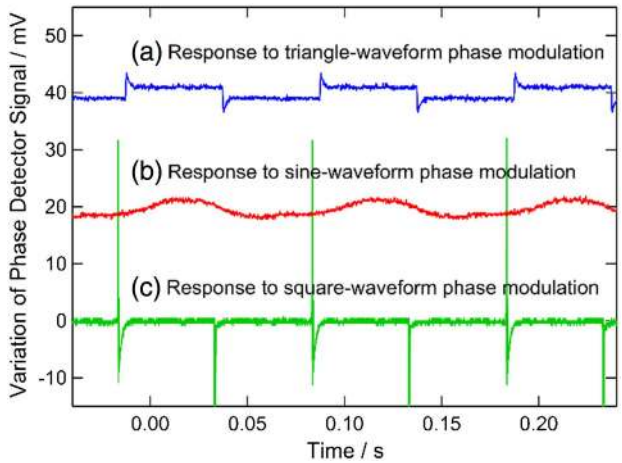

Fig. 7. Impact on RFOF transfer of phase fluctuations in the input RF reference. Responses of the RFOF phase detector to (a) triangle, (b) sine, and (c) square waveforms' phase fluctuations in RF_M and identical RF_S using 50 km of spooled fiber. Phase fluctuations in three different forms were simulated by using a signal generator.

The resulting phase-detector output of ~2° (e.g., from steps in the triangle-wave case and peak-to-peak amplitude in the sine-wave case) was found to be proportional *both* to the rate of phase fluctuations *and* to the length of the optical fiber.

Figure 7 indicates that phase variations, occurring on timescales of round-trip propagation, are indeed the major source of the observed phase fluctuations. Owing to the propagation-time delay, the RFOF transfer system cannot distinguish rapid phase-error signals arising from instability (on the timescale of the RTT) in RF_M or in fiber length. It tracks the phase of a stable RF_M, as might otherwise be expected for timescales that are long compared with the RTT. As in any time-delayed feedback servo system, RFOF systems can only act after a round-trip cycle. Short-term phase variations in RF_M, occurring on timescales of the round-trip propagation, therefore appear as a residual phase error.

These systematic laboratory-based experiments confirm the validity of our ATCA-based RFOF-characterization experiments, from which Figs. 4–6 are derived. The residual differential phase variations, observed in the split-antenna experiments (Fig. 6; black line, middle panel) and in the Allan deviation plots (i) and (ii) of Fig. 4(a) (centered at $\tau \approx 200$ s), are attributable to frequency fluctuations in the reference RF_M itself. However, they are very much smaller than the typical atmospheric variability between separate VLBI antennas.

Moreover, these laboratory-based results are consistent with and validate the algebraic formulation presented in the Appendix of our original paper [22], which presents a general algebraic description of the RFOF transfer processes.

E. General Discussion

In recent years, optical-fiber links have been widely used in major radio-astronomy facilities. For instance, the e-MERLIN array of six telescopes in the UK midlands has spanned baselines of >200 km via amplified trunk and dark optical fibers with a 1.486-GHz radio link to maintain phase stability [69]. Likewise, the Atacama Large Millimeter Array (ALMA) uses optical-fiber links between its 64 antennas that are spread over baseline separations up to 18 km, stabilized by several forms of active phase control and line-length correction [70]. Moreover, the Australia Telescope, which we have used in the present research, employs optical-fiber links to control its compact array of six antennas over baseline separations up to 6 km at ATCA [66–68].

As explained in Sections 1 and 2.A, our phase-conjugate RFOF approach [22] has demonstrated practical applications in the context of radio astronomy. In particular, it enables fiber-referenced VLBI without the need for multiple hydrogen masers. Our technique does not entail absolute timing [66], in contrast to other recent fiber-based time-and-frequency transfer schemes [2–6,9–17,28,30,31,36,42–46,50,55,64,70].

Our phase-conjugate RFOF technique [22] effectively enables realization of fiber-based radio-astronomy goals previously identified in earlier proposals [7,10,48,53–55]. We note also two recent reports of advanced techniques for optical-fiber dissemination of time and frequency references to single VLBI antennas: in Italy (over a 550-km fiber link [10] with 1.5-μm laser light locked via a frequency comb to a hydrogen maser) by Clivati *et al.* [17] and in Poland (over a 345-km fiber link with frequency-comb locking to an atomic clock) by Krehlik *et al.* [55].

By contrast, our relatively straightforward passive RFOF method [22] (Fig. 1) enables phase-coherent fiber-based transfer of a frequency reference between two widely separated VLBI antennas (115 km apart) and over a 155-km fiber-link length (Figs. 2 and 5). In this paper, we demonstrate the first application of this RFOF method for actual VLBI measurements without needing a separate hydrogen-maser reference at the remote antenna. Further, this was achieved over a much larger baseline separation (>100 km) than for ALMA [70] or ATCA [66–68] and without needing to include radio-link phase stabilization as in e-MERLIN [69].

Gozzard *et al.* very recently reported stabilized frequency-reference transfer experiments [54] at ATCA using a 77-km optical-fiber loop-back link employing one bidirectional EDFA installed in the telecom hut at Springbrook Creek and with "split-antenna" configurations similar to that used previously in our own ATCA-based experiments [24]. Their results yielded phase-difference fractional stabilities that are comparable to the fractional frequency stabilities in our Allan-deviation results [Fig. 4(a)] and provided "astronomical verification" of their frequency-reference stabilization technique [53] designed for SKA use [56–59]. By contrast, here we demonstrate actual RFOF-referenced VLBI over a very large baseline of 115 km and achieve a fractional frequency stability of 1.0×10^{-16} at $\tau \approx 2 \times 10^4$ s for an 80-MHz RF signal transferred over the 310-km link, as in Fig. 4(a); this is also well within SKA specifications [54].

4. CONCLUSIONS

For the first time to our knowledge, we have demonstrated VLBI between two widely separated radio antennas (baseline separations >100 km) using our RFOF transfer technique [22] to enable high-fidelity dissemination from a single reference-frequency source. Our RFOF transfer system yields a relative frequency stability exceeding that of two independent hydrogen masers and is significantly better than the atmospheric perturbations that usually constrain VLBI radio astronomy. Split-antenna experiments (over a "real-world" fiber-link length of 310 km) effectively eliminate atmospheric perturbations and are limited primarily by residual phase fluctuations in the ATCA references, not by the RFOF transfer technique itself.

More generally, our RFOF transfer approach [22] could facilitate reliable, cost-effective dissemination of frequency references over very long (transcontinental) distances, where the optical RTT is significant (e.g., ~100 ms over 10,000 km) but well within the phase-coherence time (>10 s) of a high-quality quartz oscillator, as used in our experiments. It is also possible for RF signals (e.g., referenced to an accurate frequency comb) to be remotely transmitted via optical fiber for other applications such as the precise calibration of environmental, industrial, and laboratory-based molecular-spectroscopic sensing.

In the context of multi-antenna VLBI radio astronomy, our RFOF transfer approach obviates the need for a remote hydrogen-maser frequency reference at every antenna location, since the measured RFOF frequency stability exceeds that of a local hydrogen maser. This inexpensive and relatively simple RFOF transfer method could therefore underpin cost-effective frequency-reference transfer for remote VLBI radio-astronomy facilities, such as the SKA [55,59–62].

Funding. Australian Research Council (ARC) (LP10100270).

Acknowledgment. The Australia Telescope Compact Array (ATCA) is part of the Australia Telescope National Facility (ATNF), which is funded by the Australian government for operation as a National Facility managed by CSIRO. AARNet provided access to the telecom data channel used for these experiments. We also thank Dr. Sascha Schediwy for useful discussions.

†Deceased.

REFERENCES

1. L.-S. Ma, P. Jungner, J. Ye, and J. L. Hall, "Delivering the same optical frequency at two places: accurate cancellation of phase noise introduced by an optical fiber or other time-varying path," Opt. Lett. **19**, 1777–1779 (1994).
2. B. Warrington, "Two atomic clocks ticking as one," Science **336**, 421–422 (2012).
3. K. Predehl, G. Grosche, S. M. F. Raupach, S. Droste, O. Terra, J. Alnis, Th. Legero, T. W. Hänsch, Th. Udem, R. Holzwarth, and H. Schnatz, "A 920-kilometer optical fiber link for frequency metrology at the 19th decimal place," Science **336**, 441–444 (2012).
4. F. Stefani, O. Lopez, A. Bercy, W.-K. Lee, Ch. Chardonnet, G. Santarelli, P.-E. Pottie, and A. Amy-Klein, "Tackling the limits of optical fiber links," J. Opt. Soc. Am. B **32**, 787–797 (2015).
5. S. Droste, T. Udem, R. Holzwarth, and T. W. Hänsch, "Optical frequency dissemination for metrology applications," C. R. Phys. **16**, 524–530 (2015).
6. O. Lopez, F. Kéfélian, H. Jiang, A. Haboucha, A. Bercy, F. Stefani, B. Chanteau, A. Kanj, D. Rovera, J. Achkar, Ch. Chardonnet, P.-E. Pottie, A. Amy-Klein, and G. Santarelli, "Frequency and time transfer for metrology and beyond using telecommunication network fibres," C. R. Phys. **16**, 531–539 (2015).
7. F. Narbonneau, M. Lours, S. Bize, A. Clairon, G. Santarelli, O. Lopez, Ch. Daussy, A. Amy-Klein, and Ch. Chardonnet, "High resolution frequency standard dissemination via optical fiber metropolitan network," Rev. Sci. Instrum. **77**, 064701 (2006).
8. M. Musha, F.-L. Hong, K. Nakagawa, and K. Ueda, "Coherent optical frequency transfer over 50-km physical distance using a 120-km-long installed telecom fiber network," Opt. Express **16**, 16459–16466 (2008).
9. D. Nicolodi, B. Argence, W. Zhang, R. Le Targat, G. Santarelli, and Y. Le Coq, "Spectral purity transfer between optical wavelengths at the 10^{-18} level," Nat. Photonics **8**, 219–223 (2014).
10. C. Clivati, G. A. Costanzo, M. Frittelli, F. Levi, A. Mura, M. Zucco, R. Ambrosini, C. Bortolotti, F. Perini, M. Roma, and D. Calonico, "A coherent fiber link for very long baseline interferometry," IEEE Trans. Ultrason. Ferroelect. Freq. Control **62**, 1907–1912 (2015).
11. P. S. Light, A. P. Hilton, R. T. White, C. Perrella, J. D. Anstie, J. G. Hartnett, G. Santarelli, and A. N. Luiten, "Bidirectional microwave and optical signal dissemination," Opt. Lett. **41**, 1014–1017 (2016).
12. C. Clivati, G. Cappellini, L. F. Livi, F. Poggiali, M. S. de Cumis, M. Mancini, G. Pagano, M. Frittelli, A. Mura, G. A. Costanzo, F. Levi, D. Calonico, L. Fallani, J. Catani, and M. Inguscio, "Measuring absolute frequencies beyond the GPS limit via long-haul optical frequency dissemination," Opt. Express **24**, 11865–11875 (2016).
13. C. Lisdat, G. Grosche, N. Quintin, C. Shi, S. M. F. Raupach, C. Grebing, D. Nicolodi, F. Stefani, A. Al-Masoudi, S. Dörscher, S. Häfner, J.-L. Robyr, N. Chiodo, S. Bilicki, E. Bookjans, A. Koczwara, S. Koke, A. Kuhl, F. Wiotte, F. Meynadier, E. Camisard, M. Abgrall, M. Lours, T. Legero, H. Schnatz, U. Sterr, H. Denker, Ch. Chardonnet, Y. Le Coq, G. Santarelli, A. Amy-Klein, R. Le Targat, J. Lodewyck, O. Lopez, and P.-E. Pottie, "A clock network for geodesy and fundamental science," Nat. Commun. **7**, 12443 (2016).
14. L. Wu, Y. Jiang, C. Ma, H. Yu, Z. Bi, and L. Ma, "Coherence transfer of subhertz-linewidth laser light via an optical fiber noise compensated by remote users," Opt. Lett. **41**, 4368–4371 (2016).
15. T. Takano, M. Takamoto, I. Ushijima, N. Ohmae, T. Akatsuka, A. Yamaguchi, Y. Kuroishi, H. Munekane, B. Miyahara, and H. Katori, "Geopotential measurements with synchronously linked optical lattice clocks," Nat. Photonics **10**, 662–666 (2016).
16. F. Riehle, "Optical clock networks," Nat. Photonics **11**, 25–31 (2017).
17. C. Clivati, R. Ambrosini, T. Artz, A. Bertarini, C. Bortolotti, M. Frittelli, F. Levi, A. Mura, G. Maccaferri, M. Nanni, M. Negusini, F. Perini, M. Roma, M. Stagni, M. Zucco, and D. Calonico, "A VLBI experiment using a remote atomic clock via a coherent fibre link," Sci. Rep. **7**, 40992 (2017).
18. C. Daussy, O. Lopez, A. Amy-Klein, A. Goncharov, M. Guinet, Ch. Chardonnet, F. Narbonneau, M. Lours, D. Chambon, S. Bize, A. Clairon, G. Santarelli, M. E. Tobar, and A. N. Luiten, "Long-distance frequency dissemination with a resolution of 10^{-17}," Phys. Rev. Lett. **94**, 203904 (2005).
19. M. Fujieda, M. Kumagai, and S. Nagano, "Coherent microwave transfer over a 204-km telecom fiber link by a cascaded system," IEEE Trans. Ultrason. Ferroelect. Freq. Control **57**, 168–174 (2010).
20. S. Pan, J. Wei, and F. Zhang, "Passive phase correction for stable radio frequency transfer via optical fiber," Photon. Netw. Commun. **31**, 327–335 (2016).
21. M. T. L. Hsu, Y. He, D. A. Shaddock, R. B. Warrington, and M. B. Gray, "All-digital radio-frequency signal distribution via optical fibers," IEEE Photon. Technol. Lett. **24**, 1015–1017 (2012).
22. Y. He, B. J. Orr, K. G. H. Baldwin, M. J. Wouters, A. N. Luiten, G. Aben, and R. B. Warrington, "Stable radio-frequency transfer over optical fiber by phase-conjugate frequency mixing," Opt. Express **21**, 18754–18764 (2013).
23. S. W. Schediwy, D. Gozzard, K. G. H. Baldwin, B. J. Orr, R. B. Warrington, G. Aben, and A. N. Luiten, "High-precision optical-frequency dissemination on branching optical-fiber networks," Opt. Lett. **38**, 2893–2896 (2013).
24. K. G. Baldwin, Y. He, B. Orr, B. Warrington, A. Luiten, P. Mirtschin, T. Tzioumis, C. Phillips, G. Aben, T. Newlands, and T. Rayner, "Dissemination of precise radio-frequency references for environmental sensing over long-haul optical-fiber networks," in *Light, Energy and the Environment*, OSA Technical Digest (online) (Optical Society of America, 2016), paper ETu3A.3.
25. M. Kumagai, M. Fujieda, S. Nagano, and M. Hosokawa, "Stable radio frequency transfer in 114 km urban optical fiber link," Opt. Lett. **34**, 2949–2951 (2009).
26. L. Zhang, L. Chang, Y. Dong, W. Xie, H. He, and W. Hu, "Phase drift cancellation of remote radio frequency transfer using an optoelectronic delay-locked loop," Opt. Lett. **36**, 873–875 (2011).
27. Ł. Śliwczyński, P. Krehlik, Ł. Buczek, and M. Lipiński, "Frequency transfer in electronically stabilized fiber optic link exploiting bidirectional optical amplifiers," IEEE Trans. Instrum. Meas. **61**, 2573–2580 (2012).
28. P. Krehlik, Ł. Śliwczyński, Ł. Buczek, and M. Lipiński, "Fiber-optic joint time and frequency transfer with active stabilization of the propagation delay," IEEE Trans. Instrum. Meas. **61**, 2844–2851 (2012).
29. C. Gao, B. Wang, W. L. Chen, Y. Bai, J. Miao, X. Zhu, T. C. Li, and L. J. Wang, "Fiber-based multiple-access ultrastable frequency dissemination," Opt. Lett. **37**, 4690–4692 (2012).
30. Ł. Śliwczyński and J. Kołodziej, "Bidirectional optical amplification in long-distance two-way fiber-optic time and frequency transfer systems," IEEE Trans. Instrum. Meas. **62**, 253–262 (2013).
31. Ł. Śliwczyński, P. Krehlik, A. Czubla, Ł. Buczek, and M. Lipiński, "Dissemination of time and RF frequency via a stabilized fibre optic link over a distance of 420 km," Metrologia **50**, 133–145 (2013).
32. Z. Wu, Y. Dai, F. Yin, K. Xu, J. Li, and J. Lin, "Stable radio frequency phase delivery by rapid and endless post error cancellation," Opt. Lett. **38**, 1098–1100 (2013).
33. P. Krehlik, Ł. Śliwczyński, Ł. Buczek, and M. Lipiński, "Multipoint dissemination of RF frequency in fiber optic link with stabilized propagation delay," IEEE Trans. Ultrason. Ferroelect. Freq. Control **60**, 1804–1810 (2013).
34. F. Yin, A. Zhang, Y. Dai, T. Ren, K. Xu, J. Li, J. Lin, and G. Tang, "Phase-conjugation-based fast RF phase stabilization for fiber delivery," Opt. Express **22**, 878–884 (2014).
35. S. Wang, D. Sun, Y. Dong, W. Xie, H. Shi, L. Yi, and W. Hu, "Distribution of high-stability 10 GHz local oscillator over 100 km optical fiber with accurate phase-correction system," Opt. Lett. **39**, 888–891 (2014).
36. F. Yin, Z. Wu, Y. Dai, T. Ren, K. Xu, J. Lin, and G. Tang, "Stable fiber-optic time transfer by active radio frequency phase locking," Opt. Lett. **39**, 3054–3057 (2014).
37. J. Wei, F. Zhang, Y. Zhou, D. Ben, and S. Pan, "Stable fiber delivery of radio-frequency signal based on passive phase correction," Opt. Lett. **39**, 3360–3362 (2014).

38. W. Li, W. T. Wang, W. H. Sun, W. Y. Wang, and N. H. Zhu, "Stable radio-frequency phase distribution over optical fiber by phase-drift auto-cancellation," Opt. Lett. **39**, 4294–4296 (2014).
39. D. Li, D. Hou, E. Hu, and J. Zhao, "Phase conjugation frequency dissemination based on harmonics of optical comb at 10^{-17} instability level," Opt. Lett. **39**, 5058–5061 (2014).
40. L. Yu, R. Wang, L. Lu, Y. Zhu, C. Wu, B. Zhang, and P. Wang, "Stable radio frequency dissemination by simple hybrid frequency modulation scheme," Opt. Lett. **39**, 5255–5258 (2014).
41. A. Zhang, Y. Dai, F. Yin, T. Ren, K. Xu, J. Li, and G. Tang, "Phase stabilized downlink transmission for wideband radio frequency signal via optical fiber link," Opt. Express **22**, 21560–21566 (2014).
42. P. Krehlik, Ł. Śliwczyński, Ł. Buczek, J. Kołodziej, and M. Lipiński, "Ultrastable long-distance fibre-optic time transfer, active compensation over a wide range of delays," Metrologia **52**, 82–88 (2015).
43. Ł. Śliwczyński and P. Krehlik, "Multipoint joint time and frequency dissemination in delay-stabilized fiber optic links," IEEE Trans. Ultrason. Ferroelect. Freq. Control **62**, 412–420 (2015).
44. Z. Jiang, Y. Dai, A. Zhang, F. Yin, J. Li, K. Xu, Q. Lv, T. Ren, and G. Tang, "Precise time delay sensing and stable frequency dissemination on arbitrary intermediate point along fiber-optic loop link with RF phase locking assistance," IEEE Photon. J. **7**, 7200809 (2015).
45. W. Chen, Q. Liu, N. Cheng, D. Xu, F. Yang, Y. Gui, and H. Cai, "Joint time and frequency dissemination network over delay-stabilized fiber optic links," IEEE Photon. J. **7**, 7901609 (2015).
46. X. Wang, Z. Liu, S. Wang, D. Sun, Y. Dong, and W. Hu, "Photonic radio-frequency dissemination via optical fiber with high-phase stability," Opt. Lett. **40**, 2618–2621 (2015).
47. L. Yu, R. Wang, L. Lu, Y. Zhu, C. Wu, B. Zhang, and P. Wang, "WDM-based radio frequency dissemination in a tree-topology fiber optic network," Opt. Express **23**, 19783–19792 (2015).
48. B. Wang, X. Zhu, C. Gao, Y. Bai, J. W. Dong, and L. J. Wang, "Square Kilometre Array Telescope—precision reference frequency synchronisation via 1f-2f dissemination," Sci. Rep. **5**, 13851 (2015).
49. R. Huang, G. Wu, H. Li, and J. Chen, "Fiber-optic radio frequency transfer based on passive phase noise compensation with frequency dividing and filtering," Opt. Lett. **41**, 626–629 (2016).
50. P. Krehlik, Ł. Śliwczyński, Ł. Buczek, J. Kołodziej, and M. Lipiński, "ELSTAB—fiber-optic time and frequency distribution technology—a general characterization and fundamental limits," IEEE Trans. Ultrason. Ferroelect. Freq. Control **63**, 993–1004 (2016).
51. X. Zhu, B. Wang, C. Gao, and L. J. Wang, "Fiber-based multiple-access frequency synchronization via 1f-2f dissemination," Chin. Phys. B **25**, 090601 (2016).
52. H. Li, G. Wu, J. Zhang, J. Shen, and J. Chen, "Multi-access fiber-optic radio frequency transfer with passive phase noise compensation," Opt. Lett. **41**, 5672–5675 (2016).
53. S. W. Schediwy, D. R. Gozzard, S. Stobie, J. A. Malan, and K. Grainge, "Stabilized microwave-frequency transfer using optical phase sensing and actuation," Opt. Lett. **42**, 1648–1651 (2017).
54. D. R. Gozzard, S. W. Schediwy, R. Dodson, M. J. Rioja, M. Hill, B. Lennon, J. McFee, P. Mirtschin, J. Stevens, and K. Grainge, "Astronomical verification of a stabilized frequency reference transfer system for the Square Kilometre Array," Astron. J. **154**, 9 (2017).
55. P. Krehlik, Ł. Buczek, J. Kołodziej, M. Lipiński, Ł. Śliwczyński, J. Nawrocki, P. Nogaś, A. Marecki, E. Pazderski, P. Ablewski, M. Bober, R. Ciuryło, A. Cygan, D. Lisak, P. Masłowski, P. Morzyński, M. Zawada, R. M. Campbell, J. Pieczerak, A. Binczewski, and K. Turza, "Fibre-optic delivery of time and frequency to VLBI station," Astron. Astrophys. **603**, A48 (2017).
56. R. Braun, T. L. Bourke, J. A. Green, E. F. Keane, and J. Wagg, *Advancing Astrophysics with the Square Kilometre Array* (SKA Organisation, 2015), pp. 1–9.
57. "SKA Project," https://www.skatelescope.org/project/.
58. "Square Kilometre Array," http://www.atnf.csiro.au/projects/ska/.
59. K. Grainge, B. Alachkar, S. Amy, D. Barbosa, M. Bommineni, P. Boven, R. Braddock, J. Davis, P. Diwakar, V. Francis, R. Gabrielczyk, R. Gamatham, S. Garrington, T. Gibbon, D. Gozzard, S. Gregory, Y. Guo, Y. Gupta, J. Hammond, D. Hindley, U. Horn, R. Hughes-Jones, M. Hussey, S. Lloyd, S. Mammen, S. Miteff, V. Mohile, J. Muller, S. Natarajan, J. Nicholls, R. Oberland, M. Pearson, T. Rayner, S. Schediwy, R. Schilizzi, S. Sharma, S. Stobie, M. Tearle, B. Wang, B. Wallace, L. Wang, R. Warange, R. Whitaker, A. Wilkinson, and N. Wingfield, "Square Kilometre Array: the radio telescope of the XXI century," Astron. Rep. **61**, 288–296 (2017).
60. E. F. Dierikx, A. E. Wallin, T. Fordell, J. Myyry, P. Koponen, M. Merimaa, T. J. Pinkert, J. C. J. Koelemeij, H. Z. Peek, and R. Smets, "White Rabbit Precision Time Protocol on long-distance fiber links," IEEE Trans. Ultrason. Ferroelect. Freq. Control **63**, 945–952 (2016).
61. "Study group on optical fiber links for UTC under the CCTF WG AFTF," https://www.ife.uni-hannover.de/fileadmin/institut/pdf/IAG-JWG-2.1/2017-05-15-16-Hannover/Hannover_may2017_Calonico_FibreSG_2.pdf.
62. "White Rabbit," http://www.ieee802.org/802_tutorials/2013-07/WR_Tutorial_IEEE.pdf.
63. M. Amemiya, M. Imae, Y. Fujii, T. Suzuyama, F.-L. Hong, and M. Takamoto, "Precise frequency comparison system using bidirectional optical amplifiers," IEEE Trans. Instrum. Meas. **59**, 631–640 (2010).
64. N. Chiodo, N. Quintin, F. Stefani, F. Wiotte, E. Camisard, Ch. Chardonnet, G. Santarelli, A. Amy-Klein, P.-E. Pottie, and O. Lopez, "Cascaded optical fiber link using the internet network for remote clocks comparison," Opt. Express **23**, 33927–33937 (2015).
65. P. G. Edwards and C. Phillips, "The long baseline array," J. Korean Astron. Soc. **30**, 659–661 (2015).
66. P. J. Hancock, P. Roberts, M. J. Kesteven, R. D. Ekers, E. M. Sadler, T. Murphy, M. Massardi, R. Ricci, M. Calabretta, G. de Zotti, P. G. Edwards, J. A. Ekers, C. A. Jackson, M. Leach, C. Phillips, R. J. Sault, L. Staveley-Smith, R. Subrahmanyan, M. A. Walker, and W. E. Wilson, "The Australia telescope 20 GHz survey: hardware, observing strategy, and scanning survey catalog," Exp. Astron. **32**, 147–177 (2011).
67. P. G. Edwards, "The Australia Telescope National Facility," J. Korean Astron. Soc. **30**, 655–657 (2015).
68. https://csiropedia.csiro.au/australia-telescope-compact-array/.
69. S. T. Garrington, B. Anderson, C. Baines, J. A. Battilana, M. N. Bentley, D. Brown, P. Burgess, P. J. Diamond, G. J. Kitching, R. McCool, T. W. B. Muxlow, R. G. Noble, N. Roddis, R. E. Spencer, and P. Thomasson, "e-MERLIN," Proc. SPIE **5489**, 332–343 (2004).
70. J.-F. Cliche and B. Shillue, "Precision timing control for radioastronomy. Maintaining femtosecond synchronization in the Atacama Large Millimeter Array," IEEE Control Syst. Mag. **26**(1), 19–26 (2006).